International Journal on
"Technical and Physical Problems of Engineering"
(IJTPE)
Published by International Organization of IOTPE

ISSN 2077-3528
IJTPE Journal
www.iotpe.com
ijtpe@iotpe.com

December 2021 | Issue 49 | Volume 13 | Number 4 | Pages 139-146

PSO-TVAC BASED OPTIMIZED FOPID CONTROLLER FOR CASCADED DC-DC BOOST CONVERTER

R. Mohajery [1] H. Shayeghi [1] J.A. Lopez Villanueva [2]

1. Energy Management Research Center, University of Mohaghegh Ardabili, Ardabil, Iran
rezamohajery76@gmail.com, hshayeghi@gmail.com
2. Department of Electronics and Computer Technology, University of Granada, Granada, Spain, jalopez@ugr.es

Abstract- DC-DC converters are widely utilized in power circuits and are essential in a variety of power electronic circuits. With a DC-DC converter control, the output voltage remains constant regardless of changes in the input/source voltage. This article designs and simulates a FOPID controller to improve the overall performance of a cascaded DC-DC boost converter. The particle swarm optimizer with the time-varying acceleration coefficients (PSO-TVAC algorithm is used to optimize the performance of FOPID and PID controllers to regulate the converter output voltage. The recommended algorithm achieves superior results while using less computing time than a basic PSO algorithm. Furthermore, a time-domain performance index called ITSE is defined as the objective function, and ISE, ITAE, and IAE are determined as evaluation functions in developing and measuring the performance of controllers. The behavior of the controllers is studied by changing the values of the input voltages in different scenarios. The transient response of the proposed system is implemented and analyzed using MATLAB/Simulink software. According to the results, the FOPID controller significantly reduces overshoot, rise, and settling time compared to the PID one.

Keywords: DC-DC Converter, Boost Converter, PSO-TVAC Algorithm, FOPID Controller.

1. INTRODUCTION

Scientific studies are extensively focusing on the usage of DC-DC converters with different output voltage values; thereby, Buck, Boost, Buck-Boost, and many other kinds of DC-DC converters have been proposed recently. DC-DC converters with high voltage conversion ratios have a broad range of applications in industrial equipment, including electric vehicles, laptop computers, vacuum discharge lamps, hydro power plants, LED drivers, and renewable energy sources such as solar cells, fuel cells, and wind turbines [1, 2]. Voltage control can be accomplished using power electronic DC-DC converters in a wide variety of applications. Developing robust and reliable controllers that also meet the transient and frequency response requirements is a difficult challenge for these converters.

In these studies, a controller design aims to generate an output voltage that will stay in a defined range of voltage fluctuation and load current step changes [3]. By adjusting the duty cycle implemented to the switching device, DC-DC converters can also step up or down the input voltage based on the specifications of the applied load [4].

Several control methods that produce a controlled voltage output were analyzed with different levels of effectiveness in recent studies. Due to the simple Implementing the proportional integral and derivative (PID) controller, it is the most often used approach in the industry [5]. But for certain topologies like the zeta converter, which is a fourth-order system, designing a PID controller is rather complicated and the model order reduction technique is utilized to regulate the converter's anti colony optimization-based PID controller [6]. It was suggested to implement a fractional order PID controller, named FOPID, into a four-switch buck-boost DC/DC converter to regulate the power output [7]. The simulation and experimental findings were indicated that the performance of the FOPID controller is superior to an integer order controller.

The use of multi-objective evolutionary algorithms to design a PID controller for buck converters has been explored in recent researches. Overall results demonstrated that a PID controller based on MNSGA-II performs better than a PID controller based on NSGA-II for conventional buck converters [8]. A cohort intelligence (CI) optimization method [9] was utilized to optimize the FOPID controller implemented in a buck converter. Furthermore, in various operating conditions, a novel controller for a boost DC-DC converter based on Particle Swarm Optimization (PSO) was presented and compared with a traditional PI controller with anti-windup. With the help of the code composer studio, the controllers of this project were implemented in the TMS320F28027 microcontroller. The results indicated that the suggested controller has superior performance in reducing the settling time and overshoot [10].

The conventional Boost converter is one of the most commonly utilized DC-DC converters. As a result, this paper presents a new structure for controlling a cascaded DC-DC boost converter using the FOPID controller.

Moreover, the particle swarm optimizer with the time-varying acceleration coefficients algorithm (PSO-TVAC) has been used to determine the optimum coefficients of the suggested FOPID controller, which is used to regulate the proposed converter output voltage level. This technique has a faster convergence rate than the conventional PSO algorithm, is more efficient at finding reasonable solutions, and requires less computing time. Aside from that, optimizing for a minimum error between the reference and the actual voltage is done by minimizing the objective function.

The Boost converter's voltage control and dynamic responsiveness are both weak while operating in open-loop mode. As a result, a closed-loop operation is preferable for appropriate voltage control and performance optimization. Thus, by using the optimized FOPID controller by PSO-TVAC, this study attempts to achieve better performance than prior methods.

This article is divided into six sections. Section 2 focuses on the concept of cascaded boost converters, and a short overview of the FOPID Controller structure is provided in section 3. Sections 4 and 5 discuss the objective function and PSO-TVAC algorithm theories. Finally, in section 6, the simulation and results are shown by analyzing the performance of a modified cascaded boost converter using FOPID and PID controllers.

2. CASCADED BOOST CONVERTER MODEL

As illustrated in Figure 1, a cascaded DC-DC Boost converter comprises two inductors, four semiconductors (three diodes and a transistor), and two capacitors. It is worth noting that the steady-state analysis of CCM operation of the converter is divided into two modes, which are both discussed in detail in the following equations. Table 1 lists the numerical values of the components of this converter [11].

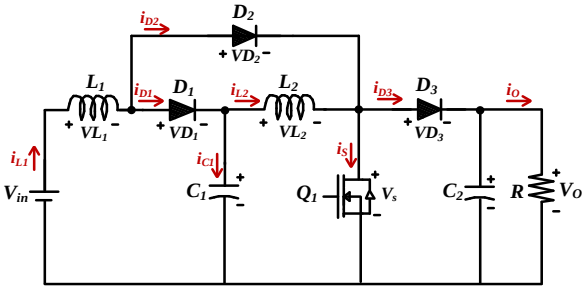

Figure 1. Cascaded boost converter with a single switch

Table 1. Parameters of the converter

Symbol	Component	Value/Model
C_1	Capacitor	22 μF
C_2	Capacitor	100 μF
L_1	Inductor	90 μH
L_2	Inductor	382 μH
R	Load Resistance	100 Ω

2.1. CCM Operation Equations

In continuous conduction mode (CCM) operation, a cascaded boost converter is stated to perform in two modes.

A MOSFET or an IGBT is used to perform the switching. MOSFET is recommended rather than IGBT in low voltage systems owing to its faster-processing speed.

Mode1 begins at t = 0 s when the transistor Q_1 and D_2 are ON, and D_1 and D_3 are OFF. The input source charges the inductor L_1, and the energy stored in the capacitor C_1 is transmitted to the inductor L_2. In addition, the output capacitor provides the necessary load energy. The direction of current flow in mode 1 is shown in Figure 2. This mode is stopped when the switch is turned OFF. As a result, the following equations are expressed:

$$V_{L1} = V_{in} \quad (1)$$

$$V_{L2} = V_C \quad (2)$$

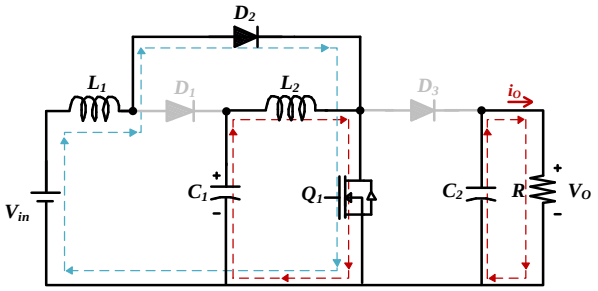

Figure 2. The current direction of mode 1

Mode 2 begins at $t = t_1$ when the transistor Q_1 and D_2 are OFF, and D_1 and D_3 are ON. The input source and the stored energy in the inductor L_1 charge the capacitor C_1 in this mode. Additionally, the energy stored in inductor L_2 is transmitted to the output capacitor, supplying the necessary energy. Figure 3 shows the direction of current flow in mode 2. This mode is stopped when the switch is turned ON. Therefore, the following equations are obtained:

$$V_{L1} = V_{in} - V_{C1} \quad (3)$$

$$V_{L2} = V_C - V_O \quad (4)$$

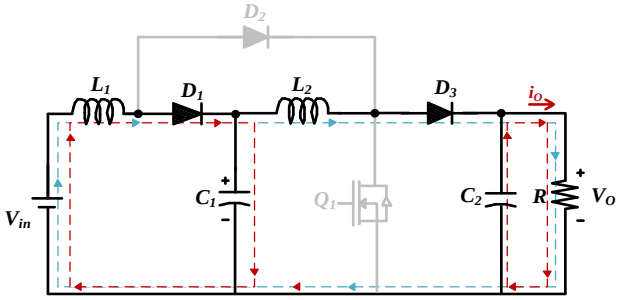

Figure 3. The current direction of mode 2

The voltage of capacitor C_1 and the converter voltage gain are determined as follows using the above equations and the volt-second law on the inductors:

$$< V_{L1} >= 0 = \frac{DT_S V_{in} + (1-D)T_S (V_{in} - V_{C1})}{T_S} \quad (5)$$

$$< V_{L2} >= 0 = \frac{DT_S V_{C1} + (1-D)T_S (V_{C1} - V_O)}{T_S} \quad (6)$$

$$V_{C1} = \frac{1}{1-D} V_{in} \tag{7}$$

$$M_{CCM} = (\frac{1}{1-D})^2 \tag{8}$$

Hence, the output voltage (V_o) will be 80 V if D = 0.5 and V_{in} = 20 V are used. As a result, the cascaded boost converter, which comprises two conventional boost converters, quadruples the output voltage.

3. FOPID CONTROLLER STRUCTURE

The construction of the fractional-order PID (FOPID) controller is a linear PID controller extension used in many applications. Figure 4 illustrates its structure. As can be seen, λ and μ are the integrator's and differentiator's fractional orders, which may range from 0 to 2 [12]. The E and U signals represent the controller's input and output, respectively. Moreover, the FOPID controller's transfer function and the output mathematical expression are given by Equations (9) and (10).

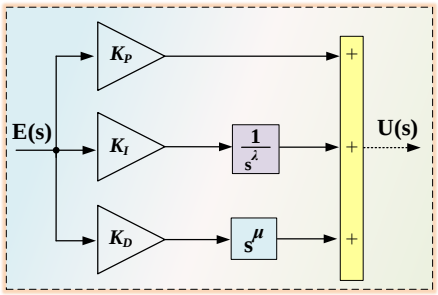

Figure 4. Structure of the FOPID controller

$$FOPID(s) = K_P + \frac{K_I}{s^\lambda} + K_D s^\mu \tag{9}$$

$$U(s) = K_P E(s) + \frac{K_I}{s^\lambda} E(s) + K_D s^\mu E(s) \tag{10}$$

K_P, K_I, and K_D represent the proportional, integral, and derivative gain coefficients. When λ and μ are set to one, the linear PID controller is achieved. Therefore, it is clear that the FOPID is an expanded form of the traditional PID controller. The FOPID controller, in contrast to the traditional PID controller, contains two more tunable parameters, which will improve the controller's flexibility while also increasing the complexity of parameter adjustment. Meanwhile, in terms of stability and dynamic performance, the proposed controller has lots of advantages. Figure 5 indicates the closed-loop control of the DC-DC converter.

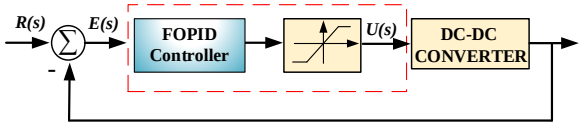

Figure 5. Representation of a DC-DC converter by a FOPID controller

4. OBJECTIVE FUNCTION

The objective function has a significant impact on the optimal tuning of the controller coefficients and the performance of the proposed DC-DC converter system.

A closed-loop control system's efficiency can be evaluated using a performance index derived from the error signal. The system parameters are modified under optimum control to reduce this index. Consequently, the intention of constructing a robust controller is to optimize responses by decreasing time-domain characteristics. In order to achieve optimal controller parameters, the objective function should be defined so that the system's dynamic response has a lower settling time and the least amount of overshoot and undershoot possible.

In this article, the integral of time multiplied by squared error (ITSE) is defined as the objective function, and the integral of squared error (ISE), integral of time multiplied by absolute error (ITAE), and the integral of absolute error are determined as evaluation functions. The following are the mathematical equations for objective and evaluation functions:

$$J_{ITSE} = \int_0^{t_{sim}} t\ e^2(t) dt \tag{11}$$

$$J_{ISE} = \int_0^{t_{sim}} e^2(t) dt \tag{12}$$

$$J_{ITAE} = \int_0^{t_{sim}} t |e(t)| dt \tag{13}$$

$$J_{IAE} = \int_0^{t_{sim}} |e(t)| dt \tag{14}$$

5. OPTIMIZATION TECHNIQUE

5.1. Particle Swarm Optimization Algorithm

The Particle Swarm Optimization (PSO) algorithm is a heuristic optimization technique inspired by simulations of simplified animal social behaviors. This strategy is based on studies into swarming phenomena like fish schooling and bird flocking. It is created for nonlinear optimization problems and has a fast calculation time and minor memory requirements [13].

A population of particles in the exploration area is randomly initialized in the PSO, much like all other population-based optimization methods. At each time step, it adjusts the trajectory of each individual toward its own best position and toward the best particle of the whole swarm to discover the global optimum solution.

The trajectory of each particle in the search space is modified in the particle swarm algorithm by dynamically adjusting the velocity of each particle based on its own flying experience and the flying experience of the other particles in the search space. In the d-dimensional search space, the equations for the position and velocity vector of the ith particle are as follows:

$$X_i = (x_{i1}, x_{i2}, x_{i3}, ..., x_{id}) \tag{15}$$

$$V_i = (v_{i1}, v_{i2}, v_{i3}, ..., v_{id}) \tag{16}$$

For each particle, the best position (that relates to the excellent fitness value attained by that particle at time t) and the particle that has been identified to be the most suited so far are as follows:

$$P_i = (p_{i1}, p_{i2}, p_{i3}, ..., p_{id}) \tag{17}$$

$$P_g = (p_{g1}, p_{g2}, p_{g3}, ..., p_{gd}) \tag{18}$$

These are then used to determine the new particle velocities and positions for the coming fitness assessment, which are represented by the following [14]:

$$v_{id} = v_{id} + c_1 \times \text{rand}(.) \times (p_{id} - x_{id}) + \\ + c_2 \times \text{Rand}(.) \times (p_{gd} - x_{id}) \quad (19)$$

$$P_i = (p_{i1}, p_{i2}, p_{i3}, ..., p_{id}) \quad (20)$$

where, c_1 and c_2 are acceleration coefficients, and rand(.) and Rand(.) are random numbers in the range [0,1].

5.2. Time-Varying Acceleration Coefficients (TVAC)

A new technique, known as PSO-TVAC, has been reported to enhance the performance and ability of the conventional PSO. It is evident from Equation (19) that the cognitive and the social component in PSO lead the search for the best solution. Hence, it is critical to properly control these two components to discover the optimal solution correctly and efficiently. Enhancing the global search and promoting particle convergence toward the global optima are significant focuses in the optimization process of this work [14].

The cognitive component is reduced while the social component is increased when the acceleration coefficients c_1 and c_2 are changed over time by the proposed method. This method can be performed using Logarithm Decreasing Inertia Weight [15], which is described in Equation (21):

$$w = w_{\max} + (w_{\min} - w_{\max}) \times \log_{10}(a + \frac{10t}{T_{\max}}) \quad (21)$$

where, $w_{\min}$ and $w_{\max}$ denote minimum and maximum inertia weight values, a is an evolutionary speed tuning constant, t shows the iteration number so far, and $T_{\max}$ presents the maximum iteration. The following is a mathematical representation of this adjustment:

$$c_1 = (c_{1f} - c_{1i}) \frac{t}{T_{\max}} + c_{1i} \quad (22)$$

$$c_2 = (c_{2f} - c_{2i}) \frac{t}{T_{\max}} + c_{2i} \quad (23)$$

where, c_{1i}, c_{1f}, c_{2i}, and c_{2f} show constant values. Figure 6 displays the flowchart of PSO-TVAC for finding parameters of the proposed controller of the converter.

5.3. Design of FOPID Controller Based on PSO-TVAC

It is considered a significant problem in this research that the suggested controller parameters in the DC-DC converter are correctly optimized. The efficient implementation of the FOPID controller depends on the exact tuning of the K_P, K_I, K_D, λ, and μ parameters.

The PSO-TVAC algorithm is used to design the suggested controller. Compared to genetic algorithm (GA) and traditional particle swarm optimization (PSO) algorithm, this approach offers considerable benefits in terms of convergence speed, discovering better solutions, and avoiding becoming stuck in the local stage.

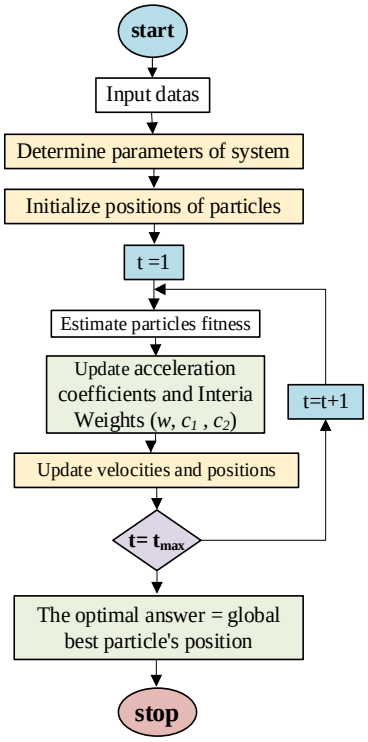

Figure 6. The PSO-TVAC flowchart

The design process for the FOPID controller with the ITSE index, utilizing the PSO-TVAC, is displayed in Figure 7. The suggested controller parameter's range of adjustments is described in Equation (24). The terms max and min in this equation denote the parameters' maximum and minimum values, respectively. The specifications of the PSO-TVAC utilized in the design process are presented in Table 2, and the optimum parameters of the FOPID and PID controllers are shown in Table 3.

$$K_P^{\min} \le K_P \le K_P^{\max}$$
$$K_I^{\min} \le K_I \le K_I^{\max}$$
$$K_D^{\min} \le K_D \le K_D^{\max} \quad (24)$$
$$\lambda^{\min} \le \lambda \le \lambda^{\max}$$
$$\mu^{\min} \le \mu \le \mu^{\max}$$

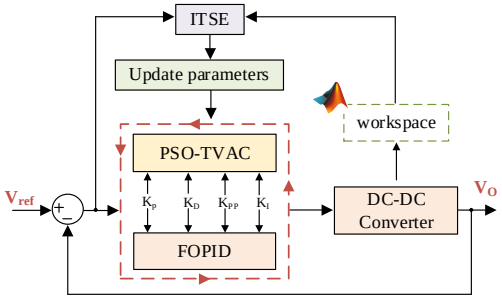

Figure 7. Algorithm-based FOPID controller design process using ITSE

Table 2. The proposed algorithm parameters

parameter	value
Population	50
Iteration	60
Lower bounds of controller parameters	0.001
upper bounds of controller parameters [K_P K_I K_D λ μ]	[2 15 2 0.999 0.999]

Table 3. Optimized Parameters of Controllers

Controller	Parameters of Controllers				
	K_P	K_I	K_D	λ	μ
FOPID	0.0026	14.9839	0.0030	0.9358	0.1246
PID	0.0031	5.951	0.0025	-	-

6. SIMULATION RESULTS AND DISCUSSIONS

To verify the effectiveness of FOPID and PID controllers, the cascaded DC-DC boost converter control structure is simulated in version 2019b of MATLAB/Simulink software on an intel-corei7/16GB DDR3 personal computer. Figure 8 presents the proposed DC-DC converter simulation, along with the suggested FOPID controller. A pulse signal for the MOSFET switch was generated using the repeating sequence block in MATLAB. Under different scenarios and circumstances, the FOPID controller's performance is compared with the PID controller.

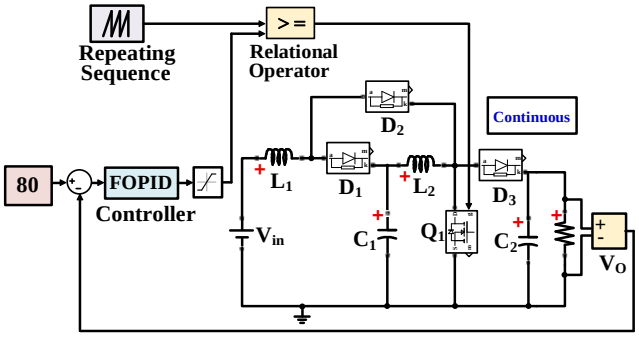

Figure 8. The suggested converter's Simulink model by FOPID

6.1. Case 1

This study simulates the proposed cascaded boost converter at a 50% duty cycle (D=0.5). The purpose of this case is to investigate the DC-DC output voltage using FOPID and PID controllers. In this scenario, the input voltage is 20 volts, and the output voltage should be 80 volts according to Equation (8). Figure 9 depicts the open-loop operation's output voltage shape. As displayed, the converter's voltage management and dynamic responsiveness are poor while operating in the open-loop system. The FOPID controller has enhanced transient response specifications, as shown in Figure 10. As a result, the proposed controller's settling time is faster than the PID controller, significantly reducing overshoot.

As measured by the objective and evaluation functions (ITSE, ISE, ITAE, IAE), the suggested controller's efficiency is shown in Figure 11. The findings demonstrate that applying the ITSE index improves the performance of FOPID.

Furthermore, the improvement percentage of the time-domain characteristics in the first scenario, including overshoot, settling, and rise time with the FOPID controller compared to the PID controller, is presented in Figure 12. So, it is concluded that the PSO-TVAC based FOPID controller has enhanced the system's dynamic behavior.

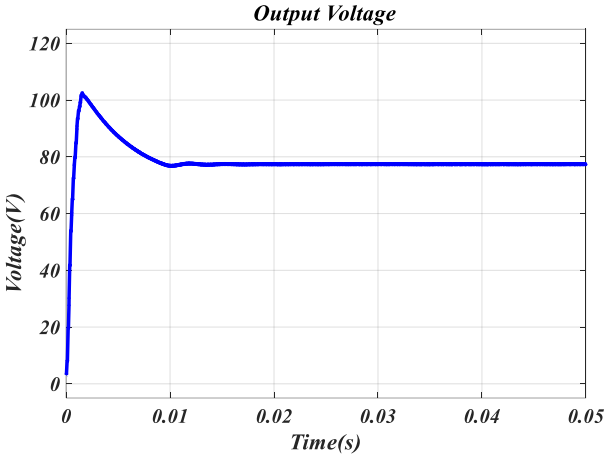

Figure 9. Output voltage of converter in the open-loop operation mode

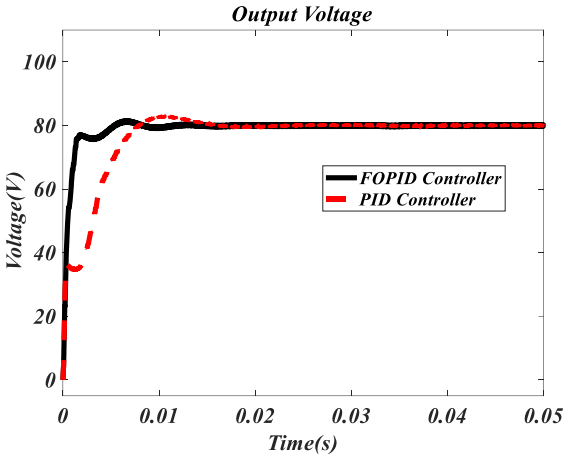

Figure 10. Output voltage shape of the cascaded converter in Case 1

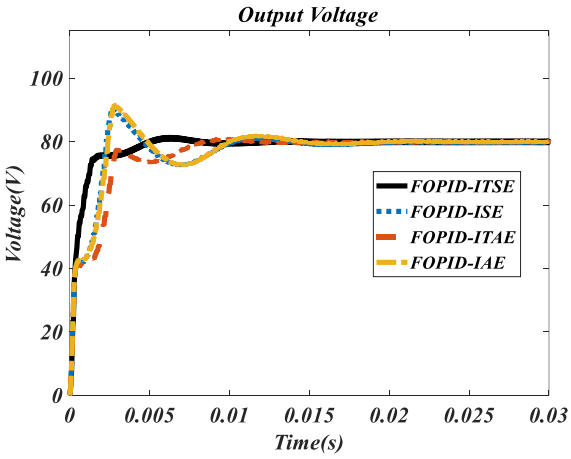

Figure 11. Suggested controller's efficiency with different objective functions

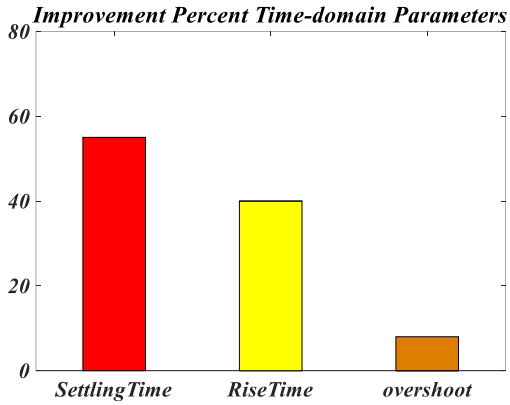

Figure 12. Time response characteristics improvement percentage in the Case 1

6.2. Case 2

The cascaded boost converter is simulated using a 25V input voltage in this scenario, and the output wave shapes are depicted in Figure 13. This scenario has been designed to ensure adequate voltage regulation of the system. It's clear that no matter what the input voltage changes, the output voltage stays constant at 80V. Despite applying voltage changes to the system, the suggested controller improves the converter's dynamic performance, and the results prove that the proposed controller effectively decreases the settling time and rise time.

Table 4 shows the time-domain characteristics in the second scenario, including overshoot, settling time, and rise time in both considered controllers. The findings indicate that the FOPID controller significantly enhances the system's dynamic behavior. Hence, its robustness is verified.

As can be seen, the controller's robustness in minimizing the variations is noticeable. In this situation, it is also shown that the system without any controller does not function well. The analysis proves that the suggested FOPID controller offers superior output voltage regulation when used in a cascaded boost converter, increasing the system's performance.

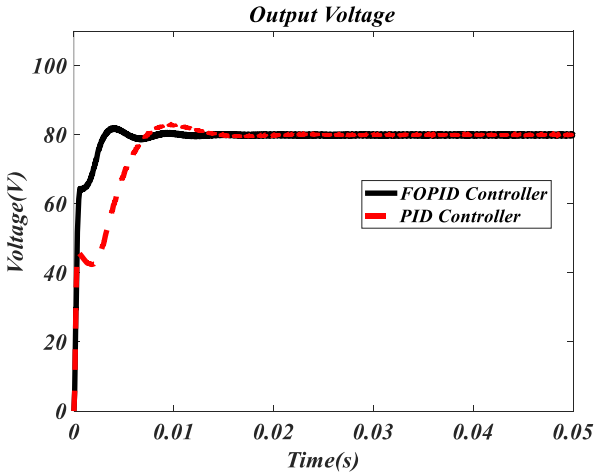

Figure 13. Output voltage shape of the cascaded converter in Case 2

Table 4. Comparison of Controllers Time-Domain Performance in the Case 2

Time-domain characteristics		Controllers	
		FOPID	PID
Overshoot	ITSE	81	87
	ISE	84	89
	ITAE	82	87.5
	IAE	86	91
Settling time	ITSE	0.008	0.017
	ISE	0.014	0.021
	ITAE	0.010	0.019
	IAE	0.015	0.024
rise time	ITSE	0.001	0.0013
	ISE	0.002	0.0025
	ITAE	0.0014	0.0018
	IAE	0.0023	0.0029

6.3. Case 3

As shown in Figure 14, this scenario analyzes the system's performance with a FOPID and PID controller under various step input voltage variations. Figure 15 represents the proposed DC-DC control's dynamic response to the step input voltage variation.

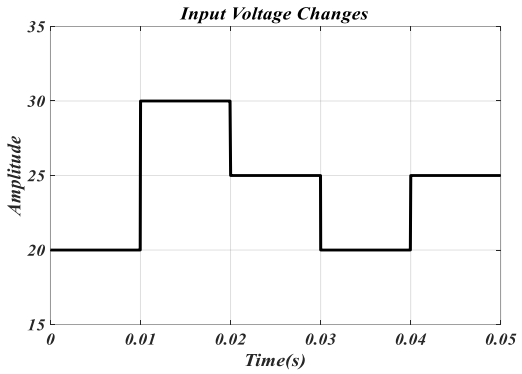

Figure 14. Step changes of the input voltage in 0.05 seconds

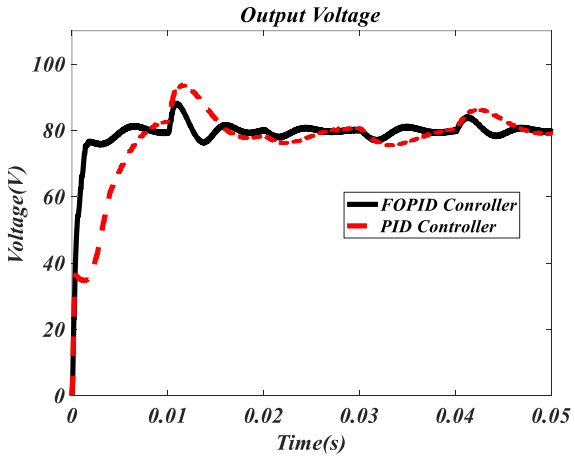

Figure 15. Output voltage shape of the cascaded converter in Case 3

7. CONCLUSIONS

This study proposes and examines the fractional-order PID (FOPID) controller performance for regulating the output voltage of a cascaded DC-DC boost converter.

Since the operation of the FOPID controller is fundamentally dependent on the appropriate optimization of the coefficients of its structure, the PSO-TVAC algorithm is used to optimize these coefficients, and the ITSE objective function is used to determine the best controller coefficients throughout the controller design process. The suggested converter provides more accurate voltage regulation with a FOPID controller, which also enhances the converter's performance. Although all of the controllers provide stabilized outputs, the suggested controller produces decreased output fluctuations. Consequently, this study effectively presents a way for satisfying the purpose of a DC-DC converter, which is to keep a steady output voltage at the load side. Moreover, the presented circuit is uncomplicated, simple, and also can be constructed without extra components. The expansion of the FOPID controller to control converters, such as boost and buck-boost converters, could be the subject of future investigations.

REFERENCES

[1] M.E. Azizkandi, F. Sedaghati, H. Shayeghi, F. Blaabjerg, "A high voltage gain DC-DC converter based on three winding coupled inductor and voltage multiplier cell", IEEE Transactions on Power Electronics, vol. 35, no. 5, pp. 4558-4567, 2019, Clerk Maxwell, A Treatise on Electricity and Magnetism, 3rd ed., vol. 2. Oxford: Clarendon, pp. 68-73, 1892.

[2] M. Eskandarpour Azizkandi, F. Sedaghati, H. Shayeghi, "An interleaved configuration of modified ky converter with high conversion ratio for renewable energy applications; design, analysis and implementation", Journal of Operation and Automation in Power Engineering, vol. 7, no. 1, pp. 90-106, 2019.

[3] T. G. Habetler, R.G. Harley, "Power electronic converter and system control", Proceedings of the IEEE, vol. 89, no. 6, pp. 913-925, 2001.

[4] M. Banaei, H. Ajdar Faeghi Bonab, N. Taghizadegan Kalantari, "Analysis and design of a new single switch non-isolated buck-boost dc-dc converter", Journal of Operation and Automation in Power Engineering, vol. 8, no. 2, pp. 116-127, 2020.

[5] C.B. Ali, A.H. Khan, K. Pervez, T.M. Awan, A. Noorwali, S.A. Shah, "High Efficiency High Gain DC-DC Boost Converter Using PID Controller for Photovoltaic Applications", International Congress of Advanced Technology and Engineering (ICOTEN), 2021: IEEE, pp. 1-7, 2021.

[6] S. Arun, T. Manigandan, "Design of ACO based PID controller for zeta converter using reduced order methodology", Microprocessors and Microsystems, vol. 81, p. 103629, 2021.

[7] Z. Qi, J. Tang, J. Pei, L. Shan, "Fractional controller design of a DC-DC converter for PEMFC", IEEE Access, vol. 8, pp. 120134-120144, 2020.

[8] M. Rajamani, R. Rajesh, M. Willjuice Iruthayarajan, "Design and Experimental Validation of PID Controller for Buck Converter: A Multi-Objective Evolutionary Algorithms Based Approach", IETE Journal of Research, pp. 1-12, 2021.

[9] P. Warrier, P. Shah, "Optimal Fractional PID Controller for Buck Converter Using Cohort Intelligent Algorithm", Applied System Innovation, vol. 4, no. 3, p. 50, 2021.

[10] O. Ibrahim, N.Z. Yahaya, N. Saad, "Comparative studies of PID controller tuning methods on a DC-DC boost converter", The 6th IEEE International Conference on Intelligent and Advanced Systems (ICIAS), pp. 1-5, 2016.

[11] J.A. Morales Saldana, R. Galarza Quirino, J. Leyva Ramos, E.E. Carbajal Gutierrez, M.G. Ortiz Lopez, "Modeling and control of a cascaded boost converter with a single switch", The 32nd Annual Conference on IEEE Industrial Electronics (IECON 2006), pp. 591-596, 2006.

[12] P. Shah, S. Agashe, "Review of fractional PID controller", Mechatronics, vol. 38, pp. 29-41, 2016.

[13] H. Shayanfar, H. Shayeghi, A. Ghasemi, "SPSO-TVAC Congestion Management in a Practical Electricity Market Based Generator Sensitivity", International Conference on Artificial Intelligence (ICAI), The Steering Committee of The World Congress in Computer Science, Computer, p. 1, 2014.

[14] A. Ratnaweera, S.K. Halgamuge, H.C. Watson, "Self-organizing hierarchical particle swarm optimizer with time-varying acceleration coefficients", IEEE Transactions on Evolutionary Computation, vol. 8, no. 3, pp. 240-255, 2004.

[15] Y.L. Gao, X.H. An, J.M. Liu, "A particle swarm optimization algorithm with logarithm decreasing inertia weight and chaos mutation", IEEE International Conference on Computational Intelligence and Security, vol. 1, pp. 61-65, 2008.

BIOGRAPHIES

Reza Mohajery was born in Ardabil, Iran, in 1998. He received the B.Sc. degree in Electrical Engineering from University of Tabriz, Tabriz, Iran in 2019. Currently, he is a Power Electrical Engineering M.Sc. student in Technical Eng. Department of the University of Mohaghegh Ardabili, Ardabil, Iran. His research interests are about renewable energy, smart grids, power electronics topology, DC-DC Converter control and applications.

Hossein Shayeghi received Ph.D. degree in Electrical Engineering from Iran University of Science and Technology, Tehran, Iran in 2006. He is currently a Full Professor and the Scientific Director of the Energy Management Research Center, University of Mohaghegh Ardabili, Ardabil, Iran. His research interests are power system control and operation, microgrid and smart grids control and energy management and FACTs device. He has authored and co-authored of 12 book chapters in international publishers and more than 430 papers in international journals and conference proceedings that received in Google Scholar more than 6275 citations with

an H-index equal to 40. He has been included in the Thomson Reuters' list of the top one percent of most-cited technical Engineering scientists in 2015-2020, respectively. He is editor-in chief of Journal of Operation and Automation in Power Engineering and Journal of Energy Management and Technology.

Juan A. Lopez Villanueva received the Ph.D. degree in Physics in 1990 from the University of Granada (Spain), where he is currently a Full Professor. His research activity has been mainly devoted to characterization, modeling and simulation of electron devices and sensors, electronic intrumentation and power electronics. He has authored and co-authored many papers in international journals and conference proceedings that received about 3000 citations with an H-index equal to 29 in Google Scholar. He has been Coordinator of Electronics Engineering and Head of the Department of Electronics and Computer Technology at the University of Granada.